A Periocolomotor Nitridergic Population in the Macaque and Cat

Jonathan T. Erichsen[1] *and Paul J. May*[2–4]

Purpose. We determined the distribution of cells containing synthetic enzymes for the unconventional neurotransmitter, nitric oxide, with respect to the known populations within the oculomotor complex.

Methods. The oculomotor complex was investigated in monkeys and cats by use of histochemistry to demonstrate nicotinamide adenine dinucleotide phosphate diaphorase positive (NADPHd$^+$) cells and antibodies to localize neuronal nitric oxide synthase positive (NOS$^+$) cells. In some cases, wheat germ agglutinin conjugated horseradish peroxidase (WGA-HRP) was injected into extraocular muscles to allow comparison of retrogradely labeled and NADPHd$^+$ cell distributions.

Results. The distribution of the NADPHd$^+$ and NOS$^+$ neurons did not coincide with that of preganglionic and extraocular motoneurons in the oculomotor complex. However, labeled perioculomotor neurons were observed. Specifically, in monkeys, they lay in an arc that extended from between the oculomotor nuclei into the supraoculomotor area (SOA). Comparison of WGA-HRP–labeled medial and superior rectus motoneurons with NADPHd staining confirmed that the distributions overlapped, but showed that the C- and S-group cells were not NADPHd$^+$. This suggested that NADPHd$^+$ cells are part of the centrally projecting Edinger-Westphal population (EWcp). Examination of the NADPHd$^+$ cell distribution in the cat showed that these cells were indeed found primarily within its well-defined EWcp.

Conclusions. Based on their similar distributions, it appears that the peptidergic EWcp neurons, which project widely in the brain, also may be nitridergic. While the preganglionic and C- and S-group motoneuron populations do not use this nonsynaptic neurotransmitter, nitric oxide produced by surrounding NADPHd$^+$ cells may modulate the activity of these motoneurons. (*Invest Ophthalmol Vis Sci.* 2012; 53:5751–5761) DOI:10.1167/iovs.12-10287

In the pigeon, neurons that stain positively with antibodies to neuronal nitric oxide synthase (NOS) or that are stained histochemically for the NOS, nicotinamide adenine dinucleotide phosphate diaphorase (NADPHd), are present in the preganglionic Edinger-Westphal nucleus (EWpg).[1] Furthermore, NOS and NADPH diaphorase are found in the pigeon ciliary ganglion, where they reside in the preganglionic terminals and postganglionic motoneurons.[1,2] In addition, NOS blockers modulate the vasodilation induced by EW stimulation, suggesting that NOS has a crucial role in the transient control of choroidal blood flow in the bird.[3] It is believed, however, that this effect is localized to the postganglionic contacts with the vasculature, not at synapses within the ciliary ganglion,[4] leaving the role of preganglionic NOS undefined. Additionally, the role of NOS in preganglionic motoneurons in EWpg clearly is not confined to just the control of choroidal vasculature, as these cells are found in the medial and lateral EWpg of birds, and both bouton-like and cap-shaped terminals in their ciliary ganglia are NADPHd-positive (NADPHd$^+$), suggesting roles in pupil and/or lens accommodation.[1,2]

While nitric oxide (NO) also has an important role in the control of choroidal vasculature in mammals, this function appears to be supported mainly by pathways through the pterygopalatine ganglion, as opposed to those extending from the EWpg through the ciliary ganglion.[5–7] The innervation of other structures within the orbit, such as the smooth muscle controlling tension in the pulley system, is nitridergic,[8] but again is controlled mainly via the pterygopalatine ganglion.[9,10] Consistent with this, the population of NADPHd$^+$ neurons in the cat and monkey ciliary ganglion is quite small, suggesting only a limited role for NO in mammalian ciliary ganglion function.[2] Furthermore, distinct NADPHd$^+$ terminals were not observed in the ciliary ganglia of these species, although a few have been described in the rat.[2,7] Nevertheless, in light of the results observed in the pigeon and the presence of a variety of peptides in preganglionic terminals in the mammalian ciliary ganglion,[11–13] we examined the mammalian preganglionic motoneuron population supplying the ciliary ganglion for evidence of nitridergic activity.

We initially chose to investigate this question in the macaque monkey because of the similarities between macaque and human eyes, and because of the clear organization of the EW in primates, as opposed to non-primate mammals. Specifically, the preganglionic motoneurons supplying the ciliary ganglion are confined largely to a well-defined nucleus (EWpg) in monkeys[14–20] and prosimians.[21] In contrast, the preganglionic motoneurons supplying the ciliary ganglion in the non-primates investigated to date are not found in a single nucleus that can be identified cytoarchitectonically (cat,[22,23] rabbit,[24] rat[20]). Subsequently, however, we also examined the distribution of NADPHd$^+$ cells in the cat, as this species has a clearly defined EW nucleus containing centrally projecting cells (EWcp), and this nucleus contains only a very small portion of the preganglionic motoneuron population.[18,20,22]

Examination of sections from macaque brains treated to reveal NADPHd showed the presence of numerous positive cells in the region of the oculomotor nucleus (III). However, only a few of these cells were located within the confines of the EWpg. Instead their distribution was reminiscent of that

From the [1]School of Optometry and Vision Sciences, Cardiff University, Cardiff, Wales, United Kingdom; and the departments of [2]Neurobiology & Anatomical Sciences, [3]Ophthalmology, and [4]Neurology, University of Mississippi Medical Center, Jackson, Mississippi.

Supported by NEI Grants EY014263 (PJM) and EY04587 (JTE).

Submitted for publication May 29, 2012; revised July 19, 2012; accepted July 23, 2012.

Disclosure: **J.T. Erichsen**, None; **P.J. May**, None

Corresponding author: Paul J. May, Department of Neurobiology & Anatomical Sciences, University of Mississippi Medical Center, 2500 North State Street, Jackson, MS 39216; pmay@umc.edu.

shown for small motoneurons that supply multiply innervated muscle fibers (MIF) in the extraocular muscles.[25,26] Consequently, we pursued this investigation further by comparing directly the distributions of NADPHd$^+$ cells and small, MIF motoneurons. An earlier report of portions of this work appeared in abstract form.[27]

Methods

The procedures used in our study were approved by the Institutional Animal Care and Use Committee at the University of Mississippi Medical Center, and were in accordance with the IOVS Rules and Regulations for the Care and Use of Animals and were in compliance with the ARVO Statement for the Use of Animals in Ophthalmic and Vision Research. A total of 9 monkeys (*Maccaca mulatta* and *fascicularis*) and 4 cats (*Felix domesticus*) of both sexes were used. Of the monkeys, 4 received tracer injections of the medial rectus and superior rectus muscles or the medial rectus only. Other tissue from these same animals was used in experiments that did not compromise the findings in our study.

For the extraocular muscle injections, 4 monkeys were sedated with intramuscular (IM) ketamine HCl (10 mg/kg) and anesthetized with isoflurane (1%–3%). Atropine (0.05 mg/kg, IM) was given to preclude overproduction of mucus, and intravenous (IV) dexamethasone (0.5 mg/kg) was given to reduce postoperative swelling. Body temperature, heart rate, and blood gas levels were monitored and maintained within normal values during the surgery. The brow area was prepared for sterile surgery, and an incision made posterior to the supraorbital ridge. The skin then was pulled forward and the orbicularis oculi muscle disinserted from the supraorbital ridge to reveal the orbital contents. The insertions of the medial ($n = 4$) and superior ($n = 2$ of the 4) recti muscles were localized, dissected free, and stabilized with a loop of suture. The muscles then were injected with a combination of (1%–2%) wheat germ agglutinin conjugated horseradish peroxidase and 10% horseradish peroxidase (WGA-HRP) by use of a 10 μL Hamilton syringe. To label motoneurons supplying the entire muscle belly, 5 to 10 μL were injected, but to label MIF motoneurons preferentially, only 3 μL were injected into the distal tip of the muscle near the scleral insertion.[25] The region then was rinsed with sterile saline, the orbicularis oculi muscle was reattached, and the wound closed with sutures. Following a 24 to 48-hour survival, the animals with muscle injections, along with 3 other monkeys and 3 cats that had not received muscle injections, were anesthetized deeply with intraperitoneal (IP) sodium pentobarbital (50 mg/kg). They then were perfused transcardially with buffered saline followed by a fixative solution containing 1.0% paraformaldehyde and 1.25% glutaraldehyde in 0.1 M, pH 7.2 phosphate buffer (PB). An additional set composed of 2 monkeys and 1 cat was perfused instead with 4.0% buffered paraformaldehyde. The brains were blocked in the frontal or sagittal plane, and postfixed for 1 to 12 hours in the same fixative used for perfusion, before being stored in PB at 4°C.

Tissue blocks from brainstems fixed with mixed aldehydes were cut on the Vibratome into 100 μm thick serial sections. Selected series of sections were reacted to reveal the presence of NADPHd$^+$ neurons. They were treated first with Triton-X-100 (0.3% in PB) and rinsed. This was followed by incubation in a solution containing 0.02% β-nicotinamide adenine dinucleotide phosphate, 0.04% nitroblue tetrazolium, and 0.3% Triton-X-100 in PB. This reaction was terminated by rinsing in 0.1 M, pH 7.2 PB. It should be noted that NADPHd$^+$ cells in the vicinity of the oculomotor nucleus were labeled clearly only in sections fixed with mixed aldehydes, not 4.0% paraformaldehyde. In cases in which the extraocular muscle had been injected with WGA-HRP, additional procedures were performed following the NADPHd protocol to localize the labeled motoneurons, as described by Perkins et al.[28]

Tissue from brainstems fixed in 4.0% paraformaldehyde was equilibrated in a 30% sucrose 0.1 M, pH 7.2 PB solution as a cryoprotectant. It then was frozen and sectioned on a sliding microtome into 80 μm sections. Selected sections were treated with 0.3% Triton-X-100 in PB, and then placed in a primary antibody solution consisting of rabbit anti-human NOS (1:10,000; Immunostar, Hudson, WI) in 1.0% bovine serum albumin (BSA) in 0.1 M, pH 7.2 PB for 24 hours at 4°C. They then were rinsed and placed sequentially in biotinylated secondary and then in avidin-conjugated horseradish peroxidase, following standard ABC kit (Vector Laboratories, Burlingame, CA) procedures. Finally, the sections were reacted in a solution containing 1.0% DAB and 0.003% H_2O_2 in 0.1 M, pH 7.2 PB. This set of sections and an adjacent, non-reacted set were mounted onto gelatinized slides. The non-reacted set was counterstained with cresyl violet. All sets then were dehydrated, cleared and coverslipped.

The distributions of labeled neurons were plotted using an Olympus BH-2 microscope (Olympus, Tokyo, Japan) equipped with a drawing tube. Examples of labeled neurons were photographed by use of a Nikon E600 microscope (Nikon, Tokyo, Japan) equipped with a Nikon DXM 1200F digital camera powered by Metamorph software (Molecular Devices, LLC, Sunnyvale, CA). The images were adjusted in Adobe Photoshop (Adobe Systems, Inc., San Jose, CA) to resemble the view seen through the objectives. The terminology used here for the EW nucleus is defined by Kozicz et al.[20]

Results

Histochemical preparation of monkey midbrain sections for NADPHd revealed a set of labeled neurons in the vicinity of III (Fig. 1). No differences were seen between the two species of macaque, so they will be described together. The low magnification views revealed a set of labeled neurons that form paired columns just off the midline in the area between, but not within, the oculomotor nuclei (Figs. 1C, 1E). These columns extend into the supraoculomotor area (SOA) that caps III. Specifically, they wrap around the dorsomedial edge of III, and are distributed widely within the SOA. Rostral to III (Fig. 1A), they are found primarily within the anteromedian nucleus (AM). At higher magnification (Figs. 1B, 1D, 1F), they appear to be relatively small neurons compared to the neighboring motoneurons within III and within adjacent Nissl-stained sections. These cells averaged three primary dendrites that showed no consistent difference in orientation at the various rostrocaudal levels pictured.

A more complete view of the distribution of the NADPHd$^+$ cell population is afforded by chartings of their locations (Fig. 2). At rostral levels (Figs. 2A, 2B), labeled cells are common within AM, but also are located dorsal, lateral, and ventral to it. At rostral and middle levels of III (Figs. 2C–F), the labeled neurons form a pair of columns in the region between the oculomotor nuclei. Each column bends laterally around the dorsomedial pole of III and disperses into the SOA. A few labeled cells spill out laterally into the reticular formation on either side of III. Only a very few cells appear to be located within the Edinger-Westphal nucleus where the preganglionic motoneurons are located (EWpg, Figs. 2D–G). At caudal levels of III, where the caudal central subdivision is present (Figs. 2G, 2H), labeled cells are not found between the two oculomotor nuclei or within this subdivision. Instead, they occupy the SOA and spread into the overlying periaqueductal gray. A separate population hugs the ventral border of the medial longitudinal fasciculus.

A portion of the NADPHd$^+$ population appeared to lie in the same region in monkeys that contains motoneurons contributing input to MIFs within the extraocular muscles: the C-group, capping the nucleus, and the S-group, sandwiched between the two oculomotor nuclei.[25,26] To determine whether these motoneurons might be NADPHd$^+$, we injected the left medial rectus muscle to label the left C-group and left superior rectus muscle to label the right S-group with the retrograde tracer, WGA-HRP. Figure 3 reveals the appearance of

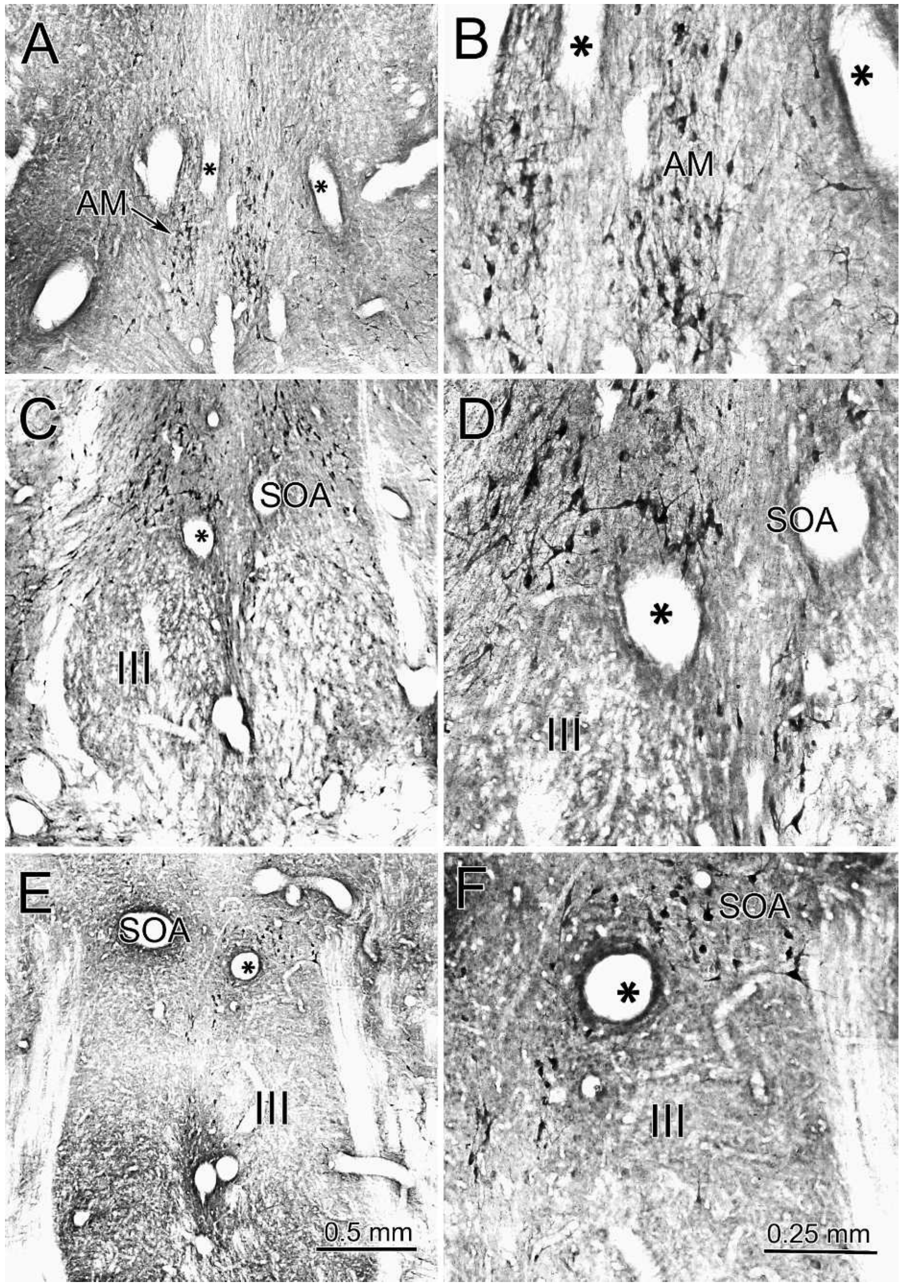

FIGURE 1. NADPHd$^+$ cells around the oculomotor nucleus of a macaque monkey. Lower magnification photomicrographs show levels located rostral (**A**) to III, near its rostral end (**C**), and midway through the nucleus (**E**). The higher magnification views from the same sections (**B**, **D**, **E**) reveal the labeled cells to be multipolar in shape with relatively small somata. The labeled cells lay between the oculomotor nuclei and spread throughout the SOA, but were not present within III itself (**C**–**F**). Rostrally, they were packed densely in the AM, but extended into the region around it. Scale in (**E**) = (**A**) and (**C**), and in (**F**) = (**B**) and (**D**). *In blood vessels, indicate the correspondence between the low and high magnification views.

the two labels (Figs. 3A–C, rostral section; Figs. 3D–F, more caudal section). Retrogradely-labeled and NADPHd$^+$ cells were apparent in sections through the rostral (Fig. 3A) and middle (Fig. 3E) portions of III. High magnification views of the C-group (Figs. 3C, 3D) showed the NADPHd$^+$ cells to be a deep purple color, while the cells containing WGA-HRP were stained reddish brown. No clearly double labeled cells were evident. Although some NADPHd crystals were present over the retrogradely-labeled cells, this artifact was present evenly throughout the tissue. The two populations appeared to overlap, although most of the MIF motoneurons tended to lie closer to III than the NADPHd$^+$ cells (Figs. 3B, 3F).

Further information on the relationship between the distributions of NADPHd$^+$ cells and MIF motoneurons can be obtained from the chartings in Figure 4. In this case, the scleral insertion of the left medial rectus was injected. Motoneurons labeled retrogradely with WGA-HRP (red squares) hugged the dorsal and dorsomedial edge of III. While their distribution overlapped with that of the cells labeled with NADPHd (dots), the latter cells had a much wider distribution, which spread across the SOA. Only a few NADPHd$^+$ cells were found within the confines of the EWpg.

Cells labeled via NADPHd histochemistry do not all necessarily use NO as a neurotransmitter. To verify our findings

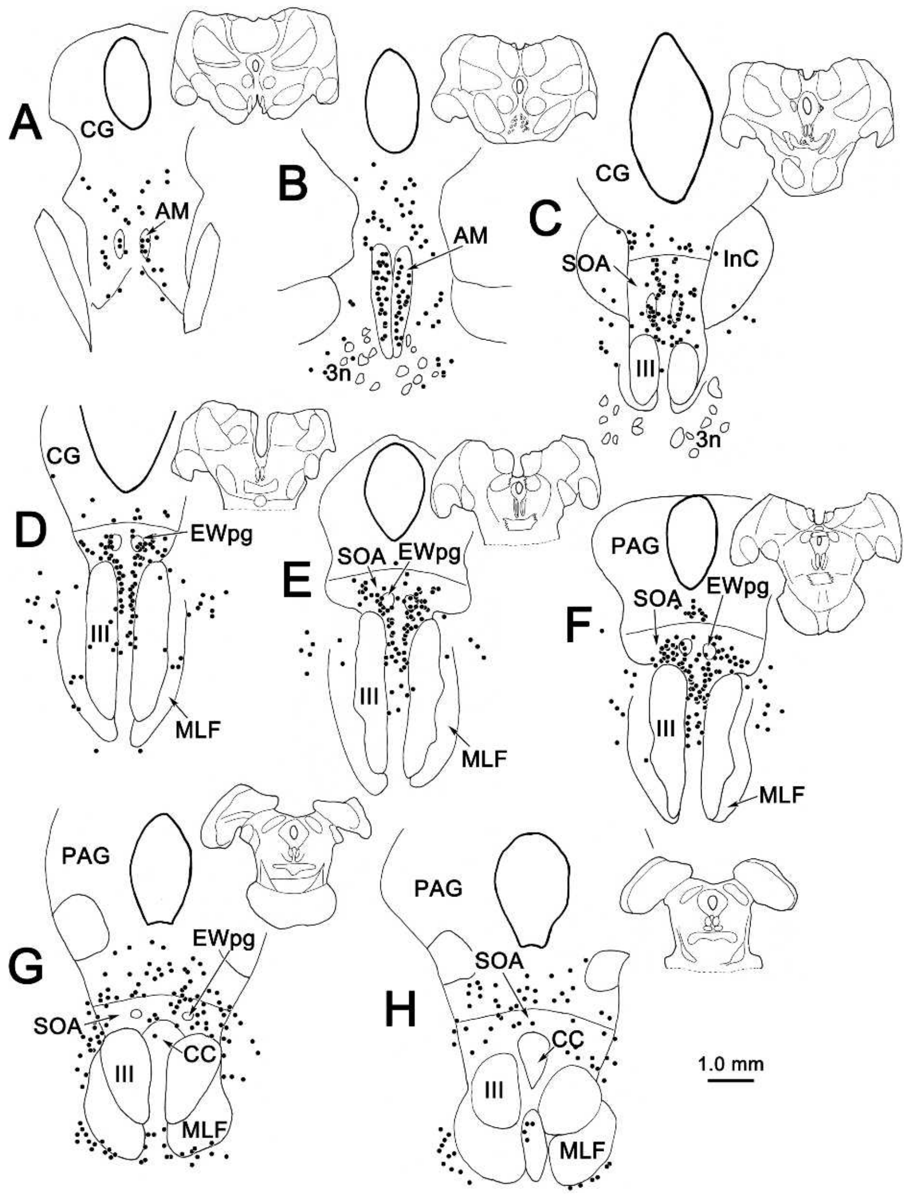

FIGURE 2. Distribution of perioculomotor NADPHd+ cells in the macaque monkey. A rostrocaudal (**A–H**) series of chartings reveals that the labeled cells (*dots*) are concentrated in the AM, but are scattered dorsal, lateral, and ventral to it (**A**, **B**). More caudally, the labeled cells form paired columns between III that arch dorsolaterally over III into the SOA, where they become more diffuse (**C–F**). A few labeled cells are present within the borders of the EWpg (**C–F**). While labeled cells occasionally were found towards the edges of III (**D**), it generally was devoid of label, as was the caudal central subdivision (CC). Other labeled cells were scattered in the periaqueductal gray (PAG) and lateral to III. CG, central gray; InC, interstitial nucleus of Cajal; MLF, medial longitudinal fasciculus; 3n, third cranial nerve.

further, we used immunohistochemistry to identify cells containing neuronal NOS in paraformaldehyde-fixed tissue. Examples of the cell labeling seen with this antibody are shown in Figure 5. The perioculomotor NOS-positive (NOS+) cells were labeled more lightly than immunopositive cells in other regions, such as the parabrachial nuclei. Nevertheless, at rostral (Figs. 5A, 5C) and caudal (Figs. 5E, 5G) levels of III, the NOS+ cells displayed the same distribution as the NADPHd+ cells, that is they lay between the oculomotor nuclei and in SOA. As can be seen by comparing the Nissl-stained (Figs. 5B, 5F) and immunohistochemically stained (Figs. 5D, 5H) sections, the NOS+ cells lie between III and EWpg as do the NADPHd+ cells. They appeared to be somewhat smaller than the motoneurons found in these adjacent nuclei (NOS+ mean long axis 12.2 μm, range 7.1–14.3 μm; EWpg mean long axis 22.6 μm, range 15–28.5 μm; III mean long axis 22.1 μm, range 17.9–28.5 μm), although this may be due to different staining characteristics.

Based on the evidence that the NADPHd+ cell population does not represent the motoneurons supplying MIF motoneurons (Figs. 3, 4), we considered a second hypothesis, that this population is equivalent to the centrally projecting Edinger-Westphal (EWcp) population of peptidergic neurons. Comparison of the present results with those from studies using antibodies to the neuropeptide urocortin-1 in the monkey reveals a very similar distribution of labeled cells.[17,18,20] Urocortin-1 is the most widespread of the neuropeptides found in this area, and is believed to have a role in controlling consumption of food and fluids, as well as in responses to stress.[20] However, the EWcp population in the macaque

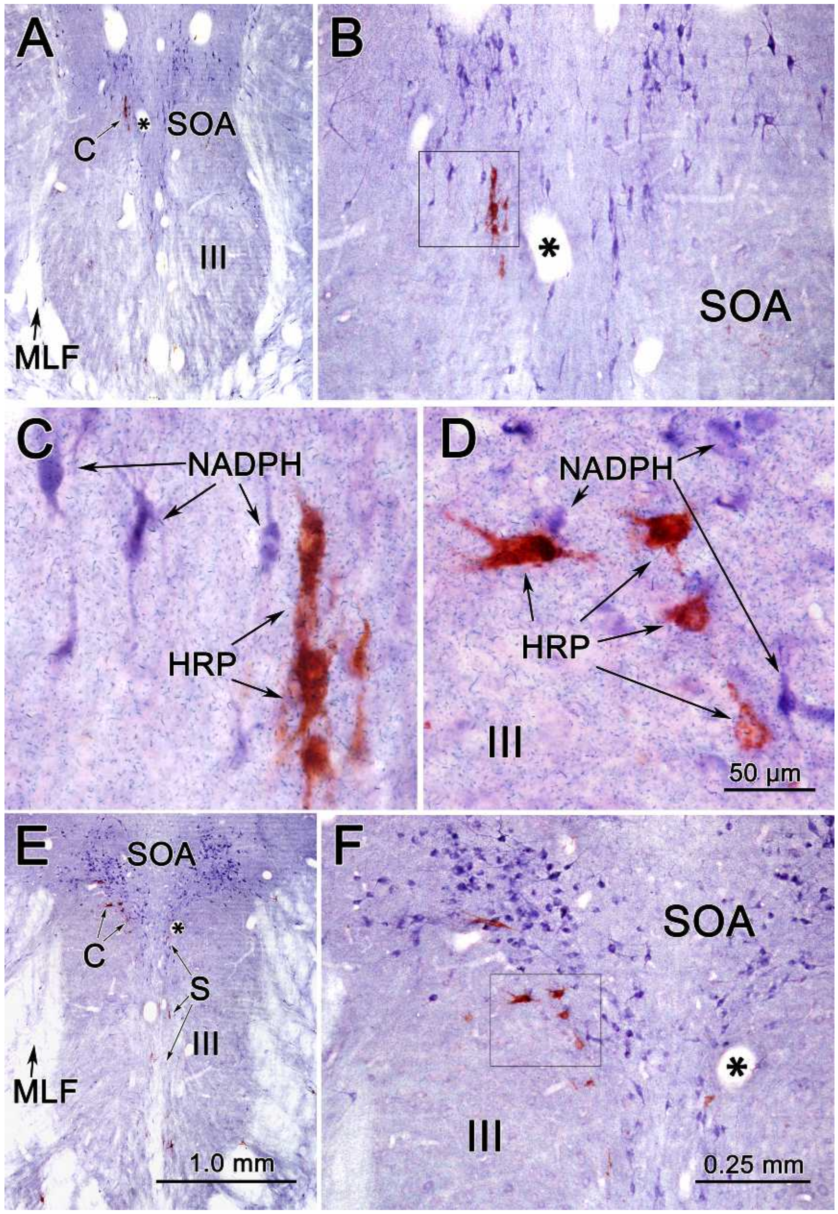

FIGURE 3. Motoneurons projecting to MIF are not NADPHd$^+$. In this monkey, the left medial and superior rectus muscles were injected with WGA-HRP, resulting in labeled cells on the left and right sides of the oculomotor complex, respectively. Since the injections were made near the muscle insertion, mainly the MIF motoneurons in the medial rectus C-group and superior rectus S-group show the reddish brown reaction product, which is discerned easily from the purple NADPHd reaction product. (**A**) and (**E**) are low magnification views through the rostral and middle levels of III. At intermediate magnifications of the same slides (**B**, **F**), the NADPHd$^+$ cells can be seen immediately adjacent to WGA-HRP labeled motoneurons. The former generally lie medial and dorsal to the latter. Higher magnification views from the regions indicated by boxes in (**B**) and (**F**) are shown in (**C**) and (**D**), respectively. They reveal that the cells in the C-group with reddish brown reaction product do not contain purple reaction product, indicating that the populations are separate. Scale in (**E**) = (**A**), (**D**) = (**C**), and (**F**) = (**B**). *In blood vessels, indicate the correspondence between the low (**A**, **E**) and higher (**B**, **F**) magnification views.

monkey does not lie in a specific nucleus, making such comparisons less precise. To test this hypothesis further, we examined the distribution of perioculomotor NADPHd$^+$ cells in the cat, where the peptidergic neurons lie primarily in a discrete EWcp nucleus. As shown in Figure 6, the vast majority of NADPHd$^+$ cells do, indeed, lie within the cat's EWcp. Small densely-labeled cells are clustered tightly within this nucleus, which is heart-shaped and located on the midline, dorsal to III (Fig. 6D). More scattered, slightly larger NADPHd$^+$ cells extend out from the nucleus into the SOA. The cells in EWcp continue forward into the anteromedian nucleus, which is found rostral to III (Figs. 6A, 6B). Once again, the cells within the nucleus are small, and densely packed, with slightly larger-appearing cells scattered laterally. There is a suggestion of separate columns for the two sides of the brain running through AM and EWcp, even though these are midline nuclei. Positive cells also were observed in the periaqueductal gray (Figs. 6A, 6C), but appeared to be a separate population.

The overall distribution of NADPHd$^+$ cells in the cat is charted in Figure 7. The labeled cells were packed closely within the midline EWcp at all levels (Figs. 7D–H). This population continues within the anteromedian nucleus rostral to III (Figs. 7B, 7C), and rostrally, even extends as two columns beyond the cytoarchitecturally defined borders of this nucleus

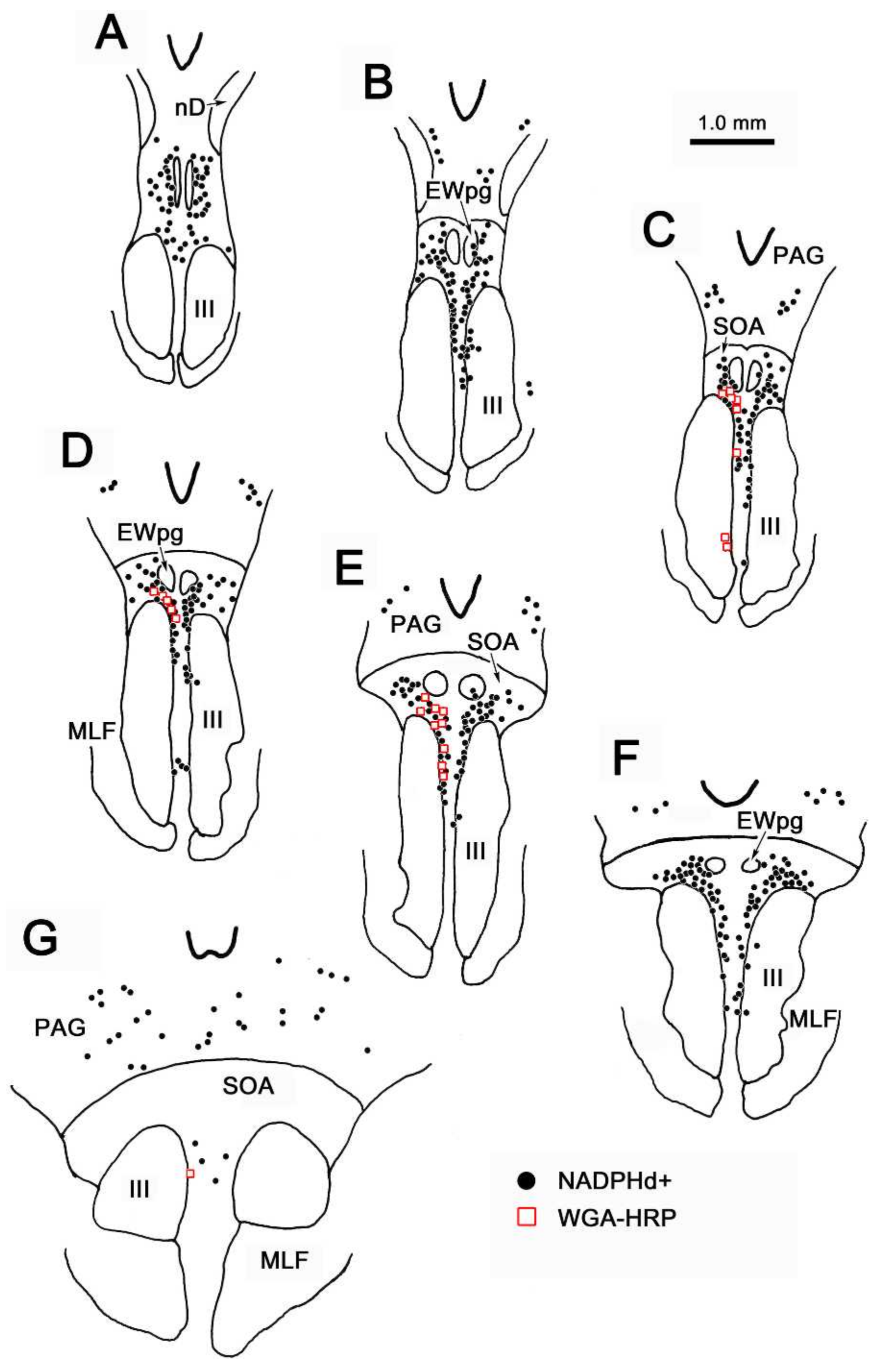

Figure 4. Distributions of motoneurons projecting to MIF in the medial rectus muscle in comparison to NADPHd$^+$ cells in the macaque monkey. A rostrocaudal (**A–G**) series of chartings indicates that the retrogradely labeled cells (*red squares*) from a muscle insertion injection of WGA-HRP almost all lie right along the dorsomedial aspect of III in C-group (**C–E**). The NADPHd$^+$ cells (*black dots*) occupy a similar territory, but extend into the SOA. A few are located at the border of the EWpg. Thus, the two labeled distributions overlap. nD, nucleus of Darkschewitsch.

(Fig. 7A). This distribution pattern correlates tightly with that of urocortin-1 in cats.[18] In addition to the NADPHd$^+$ cells found within the borders of the nuclei, other labeled cells were present between the oculomotor nuclei and in the SOA. While NADPHd$^+$ cells also were found in the periaqueductal gray and midbrain reticular formation, these cells did not appear to be part of the perioculomotor population. The use of an antibody to NOS in the cat produced a nearly identical pattern of labeling (not illustrated).

Discussion

The data from these experiments in macaque monkeys and cats indicated that a perioculomotor population of NADPHd$^+$ cells that use NOS is present in these animals. In view of the considerable evolutionary separation between these two species, it seems likely that such a population is a common feature among mammals. The distribution of these NADPHd$^+$ cells closely matches that of peptidergic populations located in

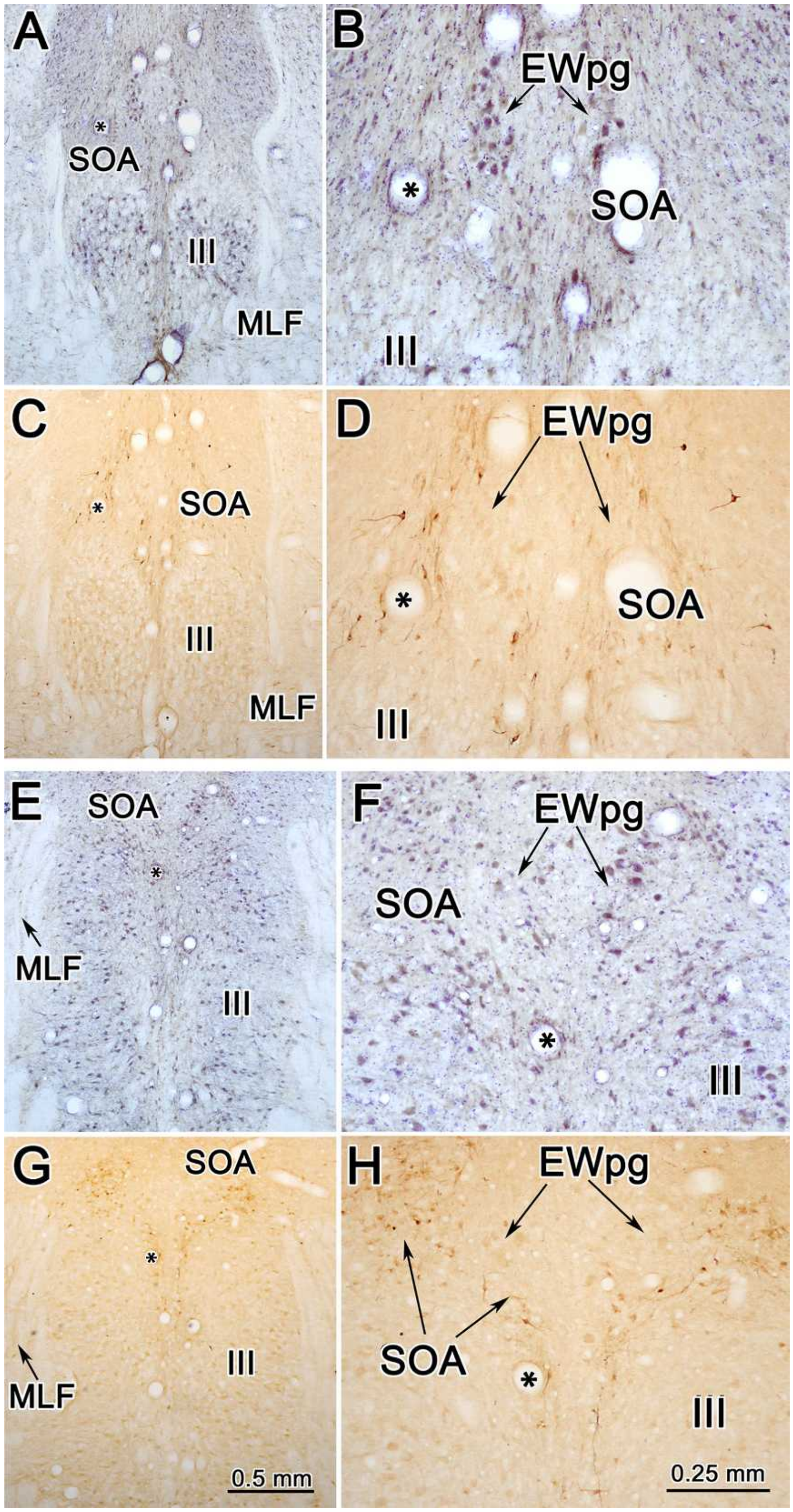

FIGURE 5. NOS+ cells in the macaque oculomotor complex. Photomicrographs show sets of sections taken through the rostral end (**A**–**D**) and middle (**E**–**H**) of III as indicated by the lower magnification views (**A**, **C**, **E**, **G**). The labeled cells are *dark brown* in color in the sections exposed to the antibody (**C**, **D**, **G**, **H**). Adjacent Nissl-stained sections are provided for comparison (**A**, **B**, **E**, **F**). The NOS+ cells can be seen arching from the midline, between III, into the SOA. Comparison of the Nissl-stained sections (**B**, **F**) to immunostained sections (**D**, **H**) reveals that these NOS+ cells were not found among the larger cells that are preganglionic motoneurons in the EWpg. Scale in (**G**) = (**A**), (**C**), (**E**), and in (**H**) = (**B**), (**D**), (**F**). *Indicate the same blood vessel in (**A**–**D**) and (**E**–**H**).

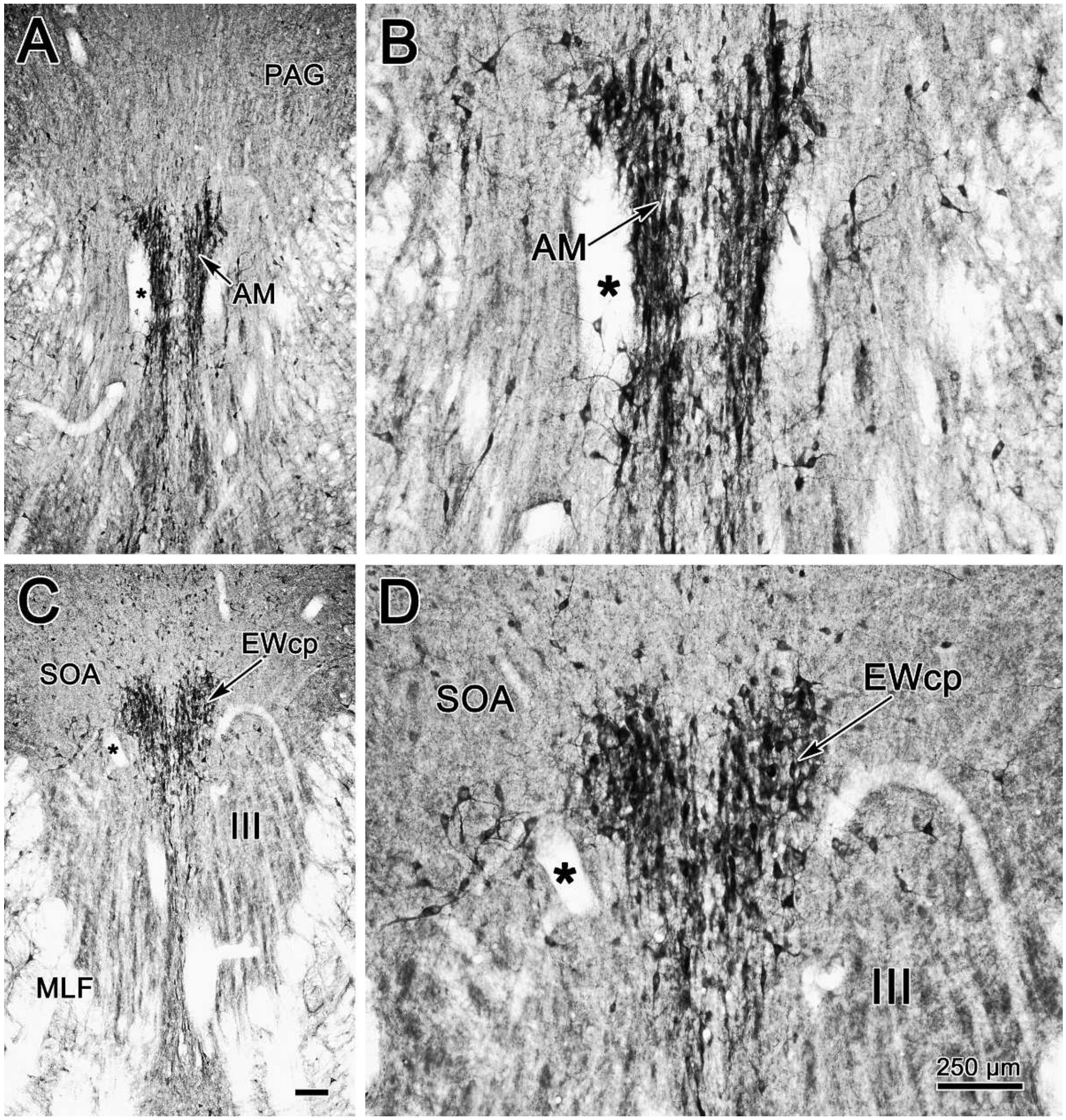

Figure 6. NADPHd+ cells in the cat oculomotor region. Sections rostral to (**A**, **B**) and in the middle (**C**, **D**) of III are shown. The AM is filled with NADPHd+ cells in the low magnification view (**A**) of the rostral section, with other labeled cells distributed dorsal and ventral to it. The higher magnification view of the same section (**B**) reveals that the labeled cells in the nucleus are slightly smaller and more fusiform than the labeled cells outside the nucleus. Caudally, most of the NADPHd+ cells lie in the centrally projecting EWcp, which lies on the midline dorsal to III (**C**). A higher magnification view of the same section (**D**) reveals that the cells in the nucleus appear slightly smaller, and much more densely packed, than the labeled multipolar cells scattered in the SOA. Both scale bars = 250 μm. Scale in (**C**) = (**A**), and in (**D**) = (**B**). *Indicate the same blood vessel in (**A**, **B**) and (**C**, **D**).

EWcp of both species.[17,18,20] In contrast, the NADPHd+ cell distribution clearly does not correspond to that of the preganglionic motoneurons supplying the ciliary ganglion, that is the EWpg, in either the monkey or cat.[14–16,18–20,22,23] While these data do not exclude the possibility that occasional preganglionic motoneurons are nitridergic, the pattern of labeling indicates strongly that the vast majority are not. These results indicated further that the distribution of the smaller NADPHd+ cells does not correspond to that of the small motoneurons supplying multiply innervated extraocular muscle fibers (MIF motoneurons) in monkeys.

Discriminating between the interneuron population in EWcp and the motoneuron population in EWpg is crucial. Earlier studies in humans assumed that a cytoarchitectonic subdivision capping III was the EW that contained preganglionic motoneurons.[29] Neurodegenerative changes observed in this nucleus in Alzheimer's sufferers[30] led to attempts to find changes in pupillary function in these patients. However, further investigation made it clear that the nucleus in question was, in fact, the EWcp, which contains peptidergic interneurons.[17,31] While it remains to be demonstrated that this population is NADPHd+ in humans, it seems highly likely in light of the present findings. The few NADPHd+ cells that were seen within the monkey EWpg were smaller in size and located near its borders, suggesting they were not truly preganglionic motoneurons. In the immunohistochemical experiments, where the borders of the EWpg were easier to define, it was even clearer that nitridergic cells were not part of the preganglionic population. This correlates well with

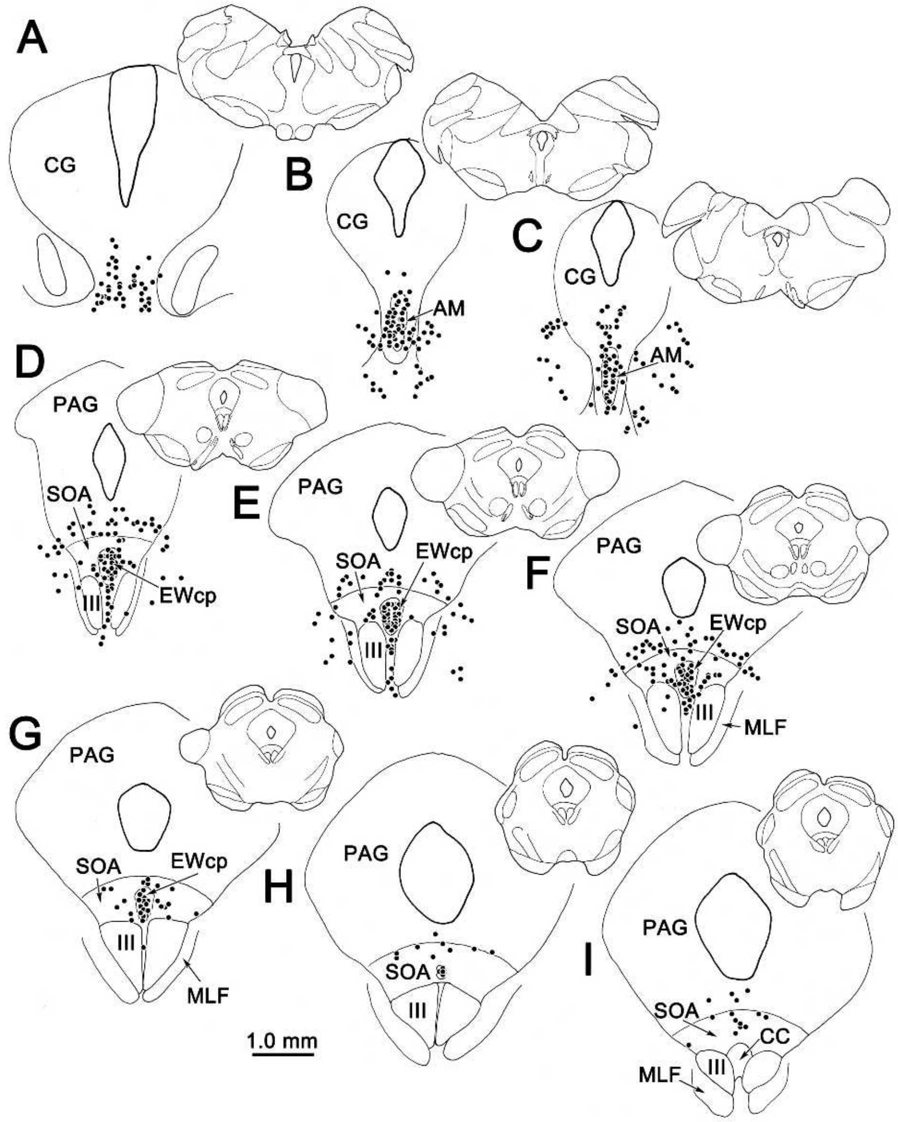

FIGURE 7. Distribution of perioculomotor NADPHd$^+$ cells in the cat. A rostrocaudal (**A–I**) series of sections is illustrated. Labeled cells (*dots*) are found in and around the anteromedian nucleus (**B**, **C**), and even extend rostral to this nucleus as paired columns (**A**). They are concentrated in the centrally projecting EWcp, but also extend laterally within the SOA and ventral to this nucleus, between III (**D–F**). Other labeled cells are scattered in the periaqueductal gray dorsal to SOA, and lateral to the MLF (**D–F**). They generally are absent from III and the CC (**I**).

the lack of NADPHd$^+$ terminals in the ciliary ganglia of monkeys[2] and humans.[9,10] Moreover, it suggests that, in primates, nitridergic modulation of activity is not a characteristic of preganglionic motoneurons or their terminals.

NADPHd$^+$ and NOS$^+$ cells also were absent from III itself in the macaques and cat, which agrees with previous reports in the cat.[32] In this regard, III appears to differ from the abducens nucleus.[32] In the cat abducens nucleus, numerous cells were NADPHd$^+$, with most appearing to be interneurons. This normally would suggest that their medial rectus targets in III should show nitridergic modification of activity. However, the oculomotor nucleus neurons in cats appear to lack NO receptors.[32] Within III, we saw no evidence of NOS immunolabeling above background levels. A small portion of NADPHd$^+$ cells in the cat abducens nucleus are motoneurons,[32] an interesting finding in light of the fact that NO influences the contractility of extraocular muscles.[33,34] However, these investigators attributed this effect to NO produced by the muscle fibers feeding back upon the motor endplates. It certainly is curious that the motoneuron population in one extraocular nucleus should contain NADPHd$^+$ cells and not the others. In contrast, we observed no NADPHd+ cells within the monkey abducens nucleus, and the few, small labeled cells seen at its borders appeared to be part of adjacent populations. This is not to say that nitridergic activity does not affect eye movements. There is extensive evidence that NO in the prepositus hypoglossi nucleus has an important role in the production of horizontal eye movements,[35–39] but an equivalent locus of nitridergic activity for the vertical gaze system has not been reported to our knowledge.

The presence of a perioculomotor population that is NADPHd$^+$ and NOS$^+$ suggested strongly that these neurons use NO in cell-to-cell communication. NO is an unconventional neurotransmitter because it is not stored in vesicles or released at synapses.[40] Instead, this small molecule diffuses out of the cell as it is manufactured and quickly influences neural activity in surrounding cells that have NOS receptors. The receptor captures the NO with a heme group and works through a guanyl cyclase to modulate cyclic GMP levels in the target cell. Since it uses a second messenger system, NO released at axonal terminals can have either excitatory or inhibitory effects on the targeted cell.[41–43] In addition, NO has been shown to act as a retrograde messenger when it is made in the postsynaptic element of a synapse. NO then diffuses back into the presynaptic element to influence future levels of synaptic release. It has been reported to have an important role in long-term potentiation and depression at synapses when used in this way.[44,45]

The degree of labeling seen in the monkey, and particularly in the cat EWcp, suggested that the vast majority of the cells in this population are producing NO. EWcp neurons already have been characterized as peptidergic based on antibody studies, with overlapping populations of cells positive for urocortin-1, substance P, cocaine and amphetamine related transcript (CART), and cholecystokinin (CCK).[17,18,31,46–49] Indeed, cells in the rat EWcp have been demonstrated to colocalize urocortin-1 and NOS.[50] Thus, it appears that, in addition to the presence of neuropeptides, these cells also produce NO. This may have important consequences if the NO is expressed in the terminals of these cells because the neurons in EWcp constitute one of the most diffusely projecting systems in the brain.[51] These projections would allow the EWcp axons to modulate activity in widely disparate brain regions using nitridergic mechanisms, up or down regulating targets based on their receptors. Alternatively, the presence of NADPHd in these cells may indicate that the EWcp cells themselves modulate the activity of their inputs. Thus, the NO they produce may allow long-term plasticity in the relationship between the firing of their inputs and their responses to those inputs. Whether NO affects the targets of the EWcp or activity in the nucleus itself, it clearly is significant for the function of this neuronal population.[20] The EWcp appears to have an important role in the control of food and fluid intake,[52–54] and also may help regulate stress responses[20] due to the similarity of urocortins to corticotropin releasing factor.

One of the striking things about the location of the NADPHd$^+$ cells is their perioculomotor location adjacent to III and the EWpg. In fact, the results indicate that these cells are intermingled with MIF motoneurons, and the dendrites of preganglionic motoneurons in EWpg must comingle with those of the nitridergic population. The SOA, which contains many of these nitrideregic cells, is believed to contain neurons whose firing is related to vergence.[55–58] Furthermore, the SOA receives axonal input from a number of gaze-related structures, including the superior colliculus, the central mesencephalic reticular formation, and portions of the deep cerebellar nuclei.[56,59–61] While it is possible that these merely are adjacent populations and the spatial relationship is not significant, it seems reasonable to suggest that the NADPHd$^+$ cell population interacts in some way with these oculomotor populations. Due to the fact that NO is a nonsynaptic neurotransmitter, it is possible that its production directly influences these surrounding cell populations. Results from an ultrastructural analysis of MIF motoneurons in our lab may be relevant in this regard. We found that these cells rarely display synapses on their somata and proximal dendrites. Perhaps this is because this nonsynaptic mode of transmission is being used to influence them (Erichsen JT, *IOVS* 1998;39:ARVO Abstract S1049). Arguing against this concept is the fact that receptors for NO were not found in the cat III.[32] However, it remains to be shown that this finding can be applied to MIF motoneurons in the monkey, which show a variety of species-specific characteristics.[25,26] Certainly, to the extent that the various behaviors tied to the EWcp represent changes in vigilance or stress levels, it would not be unreasonable for these cells to modulate the overall activity present in oculomotor neuron populations, particularly in preganglionic motoneurons controlling pupil size.

References

1. Cuthbertson S, Zagvazdin YS, Kimble TD, et al. Preganglionic endings from nucleus of Edinger-Westphal in pigeon ciliary ganglion contain neuronal nitric oxide synthase. *Vis Neurosci*. 1999;16:819–834.
2. Sun W, Erichsen JT, May PJ. NADPH-diaphorase reactivity in ciliary ganglion neurons: a comparison of distributions in the pigeon, cat, and monkey. *Vis Neurosci*. 1994;11:1027–1031.
3. Zagvazdin Y, Sancesario G, Wang YX, Share L, Fitzgerald ME, Reiner A. Evidence from its cardiovascular effects that 7-nitroindazole may inhibit endothelial nitric oxide synthase in vivo. *Eur J Pharmacol*. 1996;303:61–69.
4. Scott TR, Bennett MR. The effect of nitric oxide on the efficacy of synaptic transmission through the chick ciliary ganglion. *Br J Pharmacol*. 1993;110:627–632.
5. Bredt DS, Hwang PM, Snyder SH. Localization of nitric oxide synthase indicating a neural role for nitric oxide. *Nature*. 1990;347:768–770.
6. Bredt DS, Snyder SH. Nitric oxide, a novel neuronal messenger. *Neuron*. 1992;8:3–11.
7. Yamamoto R, Bredt DS, Snyder SH, Stone RA. The localization of nitric oxide synthase in the rat eye and related cranial ganglia. *Neuroscience*. 1993;54:189–200.
8. Demer JL, Poukens V, Miller JM, Micevych P. Innervation of extraocular pulley smooth muscle in monkeys and humans. *Invest Ophthalmol Vis Sci*. 1997;38:1774–1785.
9. Demer JL, Miller JM, Poukens V, Vinters HV, Glasgow BJ. Evidence for fibromuscular pulleys of the recti extraocular muscles. *Invest Ophthalmol Vis Sci*. 1995;36:1125–1136.
10. Gottanka J, Kirch W, Tamm ER. The origin of extrinsic nitrergic axons supplying the human eye. *J Anat*. 2005;206:225–229.
11. Kuwayama Y, Grimes PA, Ponte B, Stone RA. Autonomic neurons supplying the rat eye and the intraorbital distribution of vasoactive intestinal polypeptide (VIP)-like immunoreactivity. *Exp Eye Res*. 1987;44:907–922.
12. Leblanc GG, Trimmer BA, Landis SC. Neuropeptide Y-like immunoreactivity in rat cranial parasympathetic neurons: coexistence with vasoactive intestinal peptide and choline acetyltransferase. *Proc Natl Acad Sci U S A*. 1987;84:3511–3515.
13. Stone RA, McGlinn AM, Kuwayama Y, Grimes PA. Peptide immunoreactivity of the ciliary ganglion and its accessory cells in the rat. *Brain Res*. 1988;475:389–392.
14. Akert K, Glicksman MA, Lang W, Grob P, Huber A. The Edinger-Westphal nucleus in the monkey. A retrograde tracer study. *Brain Res*. 1980;184:491–498.
15. Burde RM, Loewy AD. Central origin of oculomotor parasympathetic neurons in the monkey. *Brain Res*. 1980;198:434–439.
16. Clarke RJ, Coimbra CJ, Aléssio ML. Distribution of parasympathetic motoneurones in the oculomotor complex innervating the ciliary ganglion in the marmoset (Callithrix jacchus). *Acta Anat (Basel)*. 1985;121:53–58.
17. Horn AK, Eberhorn A, Härtig W, Ardeleanu P, Messoudi A, Büttner-Ennever JA. Perioculomotor cell groups in monkey and man defined by their histochemical and functional properties: reappraisal of the Edinger-Westphal nucleus. *J Comp Neurol*. 2008;507:1317–1335.
18. May PJ, Reiner AJ, Ryabinin AE. Comparison of the distributions of urocortin-containing and cholinergic neurons in the perioculomotor midbrain of the cat and macaque. *J Comp Neurol*. 2008;507:1300–1316.
19. May PJ, Sun W, Erichsen JT. Defining the pupillary component of the perioculomotor preganglionic population within a unitary primate Edinger-Westphal nucleus. *Prog Brain Res*. 2008;171:97–106.
20. Kozicz T, Bittencourt JC, May PJ, et al. The Edinger-Westphal nucleus: a historical, structural, and functional perspective on

a dichotomous terminology. *J Comp Neurol*. 2011;519:1413–1434.

21. Sun W, May PJ. Organization of the extraocular and preganglionic motoneurons supplying the orbit in the lesser Galago. *Anat Rec*. 1993;237:89–103.
22. Erichsen JT, May PJ. The pupillary and ciliary components of the cat Edinger-Westphal nucleus: a transsynaptic transport investigation. *Vis Neurosci*. 2002;19:15–29.
23. Sugimoto T, Itoh K, Mizuno N. Localization of neurons giving rise to the oculomotor parasympathetic outflow: a HRP study in cat. *Neurosci Lett*. 1978;7:301–305.
24. Johnson DA, Purves D. Post-natal reduction of neural unit size in the rabbit ciliary ganglion. *J Physiol*. 1981;318:143–159.
25. Büttner-Ennever JA, Horn AK, Scherberger H, D'Ascanio P. Motoneurons of twitch and nontwitch extraocular muscle fibers in the abducens, trochlear, and oculomotor nuclei of monkeys. *J Comp Neurol*. 2001;438:318–335.
26. Wasicky R, Horn AK, Büttner-Ennever JA. Twitch and nontwitch motoneuron subgroups in the oculomotor nucleus of monkeys receive different afferent projections. *J Comp Neurol*. 2004;479:117–129.
27. May PJ, Fratkin JD. Chemoidentification of components of the oculomotor complex in macaque and man. *Soc Neurosci Abst*. 2002;28:463.16.
28. Perkins E, Warren S, Lin RC, May PJ. Projections of somatosensory cortex and frontal eye fields onto incertotectal neurons in the cat. *Anat Rec*. 288A:1310–1329.
29. Olszewski J, Baxter D. *Cytoarchitecture of the Human Brainstem*. Basel, Switzerland: S. Karger; 1982.
30. Scinto LF, Wu CK, Firla KM, Daffner KR, Saroff D, Geula C. Focal pathology in the Edinger-Westphal nucleus explains pupillary hypersensitivity in Alzheimer's disease. *Acta Neuropathol*. 1999;97:557–564.
31. Ryabinin AE, Tsivkovskaia NO, Ryabinin SA. Urocortin 1-containing neurons in the human Edinger-Westphal nucleus. *Neuroscience*. 2005;134:1317–1323.
32. Moreno-López B, Escudero M, De Vente J, Estrada C. Morphological identification of nitric oxide sources and targets in the cat oculomotor system. *J Comp Neurol*. 2001; 435:311–324.
33. Kusner LL, Kaminski HJ. Nitric oxide synthase is concentrated at the skeletal muscle endplate. *Brain Res*. 1996;730:238–242.
34. Richmonds CR, Kaminski HJ. Nitric oxide synthase expression and effects of nitric oxide modulation on contractility of rat extraocular muscle. *FASEB J*. 2001;15:1764–1770.
35. Baizer JS, Baker JF. Neurochemically defined cell columns in the nucleus prepositus hypoglossi of the cat and monkey. *Brain Res*. 2006;1094:127–137.
36. Márquez-Ruiz J, Morcuende S, de Dios Navarro-López J, Escudero M. Anatomical and pharmacological relationship between acetylcholine and nitric oxide in the prepositus hypoglossi nucleus of the cat: functional implications for eye-movement control. *J Comp Neurol*. 2007;503:407–420.
37. Moreno-López B, Escudero M, Delgado-Garcia JM, Estrada C. Nitric oxide production by brain stem neurons is required for normal performance of eye movements in alert animals. *Neuron*. 1996;17:739–745.
38. Moreno-López B, Estrada C, Escudero M. Mechanisms of action and targets of nitric oxide in the oculomotor system. *J Neurosci*. 1998;18:10672–10679.
39. Moreno-López B, Escudero M, Estrada C. Nitric oxide facilitates GABAergic neurotransmission in the cat oculomotor system: a physiological mechanism in eye movement control. *J Physiol*. 2002;540:295–306.
40. Garthwaite J. Concepts of neural nitric oxide-mediated transmission. *Eur J Neurosci*. 2008;27:2783–2802.
41. Sardo P, Carletti F, D'Agostino S, Rizzo V, Ferraro G. Effects of nitric oxide-active drugs on the discharge of subthalamic neurons: microiontophoretic evidence in the rat. *Eur J Neurosci*. 2006;24:1995–2002.
42. Schmid HA, Pehl U. Regional specific effects of nitric oxide donors and cGMP on the electrical activity of neurons in the rat spinal cord. *J Chem Neuroanat*. 1996;10:197–201.
43. Shaw PJ, Charles SL, Salt TE. Actions of 8-bromo-cyclic-GMP on neurones in the rat thalamus in vivo and in vitro. *Brain Res*. 1999;833:272–277.
44. Susswein AJ, Katzoff A, Miller N, Hurwitz I. Nitric oxide and memory. *Neuroscientist*. 2004;10:153–162.
45. Szabadits E, Cserép C, Ludányi A, et al. Hippocampal GABAergic synapses possess the molecular machinery for retrograde nitric oxide signaling. *J Neurosci*. 2007;27:8101–8111.
46. Kozicz T, Yanaihara H, Arimura A. Distribution of urocortin-like immunoreactivity in the central nervous system of the rat. *J Comp Neurol*. 1998;391:1–10.
47. Kozicz T. Neurons colocalizing urocortin and cocaine and amphetamine-regulated transcript immunoreactivities are induced by acute lipopolysaccharide stress in the Edinger-Westphal nucleus in the rat. *Neuroscience*. 2003;116:315–320.
48. Maciewicz R, Phipps BS, Foote WE, Aronin N, DiFiglia M. The distribution of substance P-containing neurons in the cat Edinger-Westphal nucleus: relationship to efferent projection systems. *Brain Res*. 1983;270:217–230.
49. Phipps BS, Maciewicz R, Sandrew BB, Poletti CE, Foote WE. Edinger-Westphal neurons that project to spinal cord contain substance P. *Neurosci Lett*. 1983;36:125–131.
50. Spina MG, Langnaese K, Orlando GF, et al. Colocalization of urocortin and neuronal nitric oxide synthase in the hypothalamus and Edinger-Westphal nucleus of the rat. *J Comp Neurol*. 2004;479:271–286.
51. Vasconcelos LA, Donaldson C, Sita LV, et al. Urocortin in the central nervous system of a primate (Cebus apella): sequencing, immunohistochemical, and hybridization histochemical characterization. *J Comp Neurol*. 2003;463:157–175.
52. Ryabinin AE, Weitemier AZ. The urocortin 1 neurocircuit: ethanol-sensitivity and potential involvement in alcohol consumption. *Brain Res Rev*. 2006;52:368–380.
53. Weitemier AZ, Ryabinin AE. Lesions of the Edinger-Westphal nucleus alter food and water consumption. *Behav Neurosci*. 2005;119:1235–1243.
54. Weitemier AZ, Ryabinin AE. Urocortin 1 in the dorsal raphe regulates food and fluid consumption, but not ethanol preference in C57BL/6J mice. *Neuroscience*. 2006;137:1439–1445.
55. Judge SJ, Cumming BG. Neurons in the monkey midbrain with activity related to vergence eye movement and accommodation. *J Neurophysiol*. 1986;55:915–930.
56. May PJ, Porter JD, Gamlin PD. Interconnections between the primate cerebellum and midbrain near-response regions. *J Comp Neurol*. 1992;315:98–116.
57. Mays LE. Neural control of vergence eye movements: convergence and divergence neurons in midbrain. *J Neurophysiol*. 1984;51:1091–1108.
58. Mays LE, Porter JD, Gamlin PD, Tello CA. Neural control of vergence eye movements: neurons encoding vergence velocity. *J Neurophysiol*. 1986;56:1007–1021.
59. Grantyn A, Grantyn R. Axonal patterns and sites of termination of cat superior colliculus neurons projecting in the tecto-bulbo-spinal tract. *Exp Brain Res*. 1982;46:243–256.
60. Harting JK. Descending pathways from the superior colliculus: an autoradiographic analysis in the rhesus monkey (Macaca mulatta). *J Comp Neurol*. 1977;173:583–612.
61. May PJ, Horn AKE, Mustari MJ, Warren S. Central mesencephalic reticular formation projections onto oculomotor motoneurons. *Soc Neurosci Abst*. 2011;37:669.04.